RESEARCH ARTICLE

# Study the Effect of Polymers Type on Preparation and Characterization of Etoposide-loaded Gold Nanoparticles

Maha M. Ali[1], Wissam S. Mahmod[2], Afaq M. Ali[3]

[1]*Department of Dental, Hilla University College, Babylon, Iraq.*
[2]*Department of Pharmaceutics, College of Pharmacy, Al-Kitab University, Altun Kupri, Iraq.*
[3]*Department of Pharmacy, Al-Rasheed University College, Baghdad, Iraq.*

***Received: 16th February, 2023; Revised: 20th March, 2023; Accepted: 24th May, 2023; Available Online: 25th June, 2023***

**ABSTRACT**

In the last few years, the discoveries in pharmaceutical nanotechnology have triggered a revolution in the field of therapeutic, delivering an abundance of novel applications and actual approaches of metallic nanoformulations for the treatment and diagnosis of tenacious diseases. From this point of view, gold nanoparticles (GN) have been awarded an attractive platform for the development of efficient multifunctional therapeutic, controlled release systems, targeted delivery and diagnostic. The objective of this research was to prepare etoposide-loaded gold nanoparticles (E-GN) by incorporating of etoposide in to the functionalized GN by using different biocompatible polymers. In the present study, GN suspension was prepared by inverse citrate reduction method. Polymeric suspensions 19 (PGN 1-19) were prepared and characterized by atomic force microscopy measurement (AFM). The obtained results indicated that PGN10, PGN13, PGN17 and PGN19 with the preferable polymers and their concentration of (1-mg/mL HPMC-E5, 1-mg/mL PVA, 1.5 mg/mL gelatin and 0.5: 0.5 mg/mL of HPMC-E5: PVA combination) respectively, showed the better morphology, particles size (PS), and particles size distribution (PSD). Subsequently, eight formulas were prepared and optimized through the study of various variables as PS, PSD, etoposide loading efficiency (LE) and *in-vitro* dissolution profile. F7 revealed a greater LE of 99.39% with higher loading capacity (1 mg/mL) and *in-vitro* dissolution with controlled mode also, AFM results showed smooth surface nanoparticles, average PS (24.43 nm) with uniform PSD (9.84%). In addition, the result of transmission electron microscopy (TEM) revealed a spherical uniform shape with zeta potential of -34.13. In conclusion, polymeric functionalization of GN improved the etoposide loading efficiency and capacity and controlled the *in-vitro* dissolution profile and enhanced their colloidal stability.

**Keywords:** Etoposide, Gold nanoparticles, Polymer, Inverse method, Particles size, Distribution.

International Journal of Drug Delivery Technology (2023); DOI: 10.25258/ijddt.13.2.39

**How to cite this article:** Ali MM, Mahmod WS, Ali AM. Study the Effect of Polymers Type on Preparation and Characterization of Etoposide-loaded Gold Nanoparticles. International Journal of Drug Delivery Technology. 2023;13(2):713-721.

**Source of support:** Nil.

**Conflict of interest:** None

## INTRODUCTION

Medical nanotechnology exhibits new scope, tools and opportunities that are prospected to have fundamental applications in therapeutics and diagnostics of diseases.

The conventional drugs challenges are recognized by poor bio-distribution, lack of selectivity, restricted effectiveness and unwanted adverse effects. Strategies that transferred drugs in to nano range, exhibit unique physic-chemical and biological characteristics, which can potentially overcome these drawbacks by: enhance surface area, increase solubility, enhance dissolution rate, decrease patient to patient and fed/fasted variability, increase oral bioavailability, prolong drug circulation (protection versus fast degradation or clearance), more rapid onset of therapeutic action, improve drug localization and targeting ability, reduce the dose required, enhance drug efficacy, decrease toxicity, decrease drug resistance and enhance the drug and formulation stability.[1]

The great interest for GN develops owing to their essential features, especially simple set up for synthesizing, easy surface functionalization, strong absorption and scattering properties, high chemical and biological stability, limited toxicity and biocompatibility.[2]

Etoposide is a powerful chemotherapy approved by the FDA as a first-line treatment of small-cell lung carcinoma (SCLC). As well as it is one of the most active agents in refractory testicular carcinoma, choriocarcinoma, neurocarcinoma, lymphoma and non-lymphatic leukemia. It inhibits cell growth mainly via inhibition of topoisomerase II enzyme resulting in DNA double-strand breaks and by the formation of free radicals.[3] Etoposide belongs to Biopharmaceutical Classification System Class-IV, has low aqueous solubility, erratic oral bioavailability 25 to 76%, as well as the peak plasma concentration ($C_{max}$) and area under the curve (AUC) exhibit marked inter- and intra-subject variability. The consequences are considerable risks of

**Author for Correspondence: mahamahdiali@gmail.com*

under-dosing and unpredictable toxicity. Therefore, an effective delivery system is required to vanquish these drawbacks and enhance its therapeutic activities.[4]

Current research aimed to improve an E-GN by using different biocompatible polymers, with high colloidal stability, LE and control dissolution profile to enhance etoposide therapeutic efficacy and selectivity.

## MATERIALS AND METHODS

Etoposide powder (98-105%), Hydrogen tetrachloroaurate trihydrate ($HAuCl_4.3H_2O$>99%) and trisodium citrate dihydrate ($Na_3C_6H_5O_7.2H_2O$>99%) were purchased from Sigma-Aldrich Co., USA. Hydroxy propyl methyl cellulose E5 (HPMC-E5) and E15 (HPMC-E15) were supplied from Provizer Pharma Co., India. Poloxamer 188 was supplied from Avonchem, UK. Poloxamer 407 was supplied from Saybronic, Actico, Jordan. Polyvinyl alcohol (PVA) was obtained from Panreac, Espana. Polyethelene glycol 200 (PEG 200) and 400 (PEG 400) were supplied from Fluka Chemi AG, Switzerland. Polyvinyl pyrrolidone 30K (PVP) was supplied from Hi media, India. Gelatin was supplied from Medichem Enterprice Co. Limited, China. All other ingredients used in the research were analytical grade.

### Methods

*Preparation of GN*

The colloidal GN was prepared by inverse citrate reduction method, using hydrogen tetrachloroaurate trihydrate as a precursor and trisodium citrate dihydrate as a mild reducing, capping, stabilizing and pH mediating agent.[5]

The preparation of GN suspension was performed by diluting 4 mL of (500 mM) citrate solution with 194 mL of preheated deionized water (DW) in a tightly sealed conical flask on a magnetic stirrer. The solution was stirred at 1500 rpm for 15 minutes at 65°C (adjusted by thermometer). Then, 2 mL of the freshly prepared (50 mM) gold solution was transferred quickly with continuous stirring at a constant temperature until a distinguishing red color was shown, indicating the GN formation. Then, switched off the heating and allowed the suspension to cool at 25°C with constant stirring, then filtered via 0.1 µm syringe-filter to expel any possible aggregates or dust impurities and stored at 2 to 8°C in a dark tightly sealed container coated with aluminum foil, to quench any reaction could be happened due to the effects of temperature or light, before further evaluation.[6]

GN strongly adhere to glass therefore, all the glass ware and magnetic beads used were treated with copious amount of a freshly prepared aqua regia solution (one part of nitric acid to three parts of hydrochloric acid) for at least one hour and thoroughly washed three times with deionized water to prevent contamination between samples and between successive synthesis processes, then dried in oven prior to their usage. All solutions were prepared by the same DW.

*Functionalization of GN suspension*

The prepared GN suspension was functionalized, as shown in Table 1, by bioconjugation method, to enhance GN's dispersing capacity and increase etoposide loading.

Nine polymeric suspensions (PGN1-9) were prepared using nine types of polymers (HPMC-E5, HPMC-E15, poloxamer 188, poloxamer 407, PVA, PEG 200, PEG 400, PVP 30K and gelatin), respectively.

Firstly, polymer solutions of HPMC-E5, HPMC-E15, poloxamer 188, poloxamer 407, PVA and gelatin were prepared at a concentration of 5 mg/mL in DW, while PEG 200, PEG 400 and PVP 30K solutions were prepared at concentration 2.5 mg/mL in DW, by mixing vigorously using a magnetic stirrer at 1500 rpm for three hours to form a homogeneous mixture. Then after, PGN suspensions were prepared by mixing 0.5 mL of each polymer solution with 4.5 mL of GN suspension separately, in a tightly sealed conical flask, for one hour at 25°C and 1500 rpm, and then sonicated for 6 hours to improve the polymer coating during the bioconjugation process.[7]

Nine suspensions (PGN10-18) were prepared from a three best types of polymer solutions (HPMC, PVA and gelatin) by mixing the GN suspension with polymeric solution in three different concentrations (10, 15 and 20 mg/mL). PGN19 containing a combination of a two synthetic polymers (HPMC-E5 and PVA) was prepared at ratio 1:1.

All the functionalized suspensions (PGN1-19) were filtered using 0.1 µm syringe-filter to expel any possible aggregates and the un-conjugated polymers, and then stored in at 2 to 8°C in a dark tightly sealed container coated by aluminum foil for further studies.[6]

AFM analysis was applied to conclude the polymer layer binding on the GN surface and infer the bio-conjugate stability to evaluate the polymer effect on the GN morphology and growth. Fourier transform infrared spectroscopy (FTIR) study was achieved to detect any sign of interaction between etoposide and polymers used in the preparation of the E-NG suspensions.

*Preparation of E-GN*

Eight formulas of medicated GN with various concentrations of etoposide, as shown in Table 2, were prepared by adding etoposide in the last step of nanoparticle preparation. Etoposide stock solution was prepared at a concentration of 15 mg/mL by dissolving 0.15 gm of etoposide in 0.5 mL of dimethyl sulfoxide (DMSO) and then completed the volume to 10 mL by a buffer solution; sonicated for about three hours at 25°C untill clear solution was obtained.

E-GN suspensions were prepared by adding 1-mL of etoposide solution to 9 mL of PNG suspension (HPMC-E5, PVA, or HPMC-E5: PVA), in a tightly sealed conical flask, and vigorously mixed for one hour on a magnetic stirrer at 1500 rpm. Subsequently, the magnetic stirrer was switched off and the medicated suspension sonicated for 5 hours till a transparent clear suspension was achieved, then stored at 2–8°C in a dark tightly sealed container coated by aluminum foil, before further analysis and evaluation.[7]

AFM was applied to measure the polymers type effect on E-GN morphology, PS and PSD. The TEM image and zeta potential of the selected formula were characterized to

**Table 1:** PGN suspensions composition

| *Sample* | *Polymer* | |
|---|---|---|
| | *Type* | *Concentration (mg/mL)* |
| PGN1 | HPMC-E5 | 5 |
| PGN2 | HPMC-E15 | 5 |
| PGN3 | poloxamer 188 | 5 |
| PGN4 | poloxamer 407 | 5 |
| PGN5 | PVA | 5 |
| PGN6 | PEG 200 | 5 |
| PGN7 | PEG 400 | 5 |
| PGN8 | PVP 30K | 5 |
| PGN9 | Gelatin | 5 |
| PGN10 | | 10 |
| PGN11 | HPMC-E5 | 15 |
| PGN12 | | 20 |
| PGN513 | | 10 |
| PGN614 | PVA | 15 |
| PGN715 | | 20 |
| PGN516 | | 10 |
| PGN517 | Gelatin | 15 |
| PGN518 | | 20 |
| PGN19 | HPMC-E5:PVA | 5:5 |

interpret the exact PS and shape of E-GN and to confirm its colloidal stability.

*Evaluation of etoposide LE*

The amount of etoposide loaded onto PGN was quantified by an indirect method, using Amicon ultra centrifugal filter of 3 KDa/MWCO (kilo Dalton / molecular weight cut-off). 0.5 mL of each E-GN suspension was centrifuged with Amicon-filter, at 6000 rpm for 20 minutes, the unbounded etoposide passed through the filter. UV-vis measurements detected the free etoposide amount. The LE of etoposide was calculated via following equation:

$$\boldsymbol{E}_{\%} = \frac{D_0 - D_f}{D_0} \times 100\%$$

Where:

$LE_{\%}$ is the loading efficiency percentage of drug.

$D_0$ is the drug total amount that fed initially to prepare a formula.

$D_f$ is the free drug amount that leak via centrifugal filter.

All drug LE studies were repeater in triplicates. The results were presented in mean value ± standard deviations.[8]

*Evaluation of In-vitro etoposide release*

The *in-vitro* release of etoposide from the E-GN suspensions was performed according to the USP Type II paddle apparatus, using cellulose diffusion dialysis membrane consisted 12 KDa/MWCO pore size.

**Table 2:** E-GN formulas composition

| *Formula* | *Polymer type* | *Temperature (°C)* | *pH of etoposide stock solution* | *Final Etoposide concentration (mg/mL)* |
|---|---|---|---|---|
| F1 | HPMC-E5 | 25 | 4.6 | 0.5 |
| F2 | PVA | 25 | 4.6 | 0.5 |
| F3 | Gelatin | 55 | 10.5 | 0.5 |
| F4 | HPMC-E5:PVA | 25 | 4.6 | 0.5 |
| F5 | Gelatin | 55 | 10.5 | 1 |
| F6 | Gelatin | 55 | 10.5 | 1.5 |
| F7 | HPMC-E5:PVA | 25 | 4.6 | 1 |
| F8 | HPMC-E5:PVA | 25 | 4.6 | 1.5 |

A volume of 20 mL of each suspension was putted in dialysis diffusion tube; with tied ends, then immersed in a dissolution jar filled with 500 mL dissolution medium maintained at a constant experimental temperature 37 ± 1°C. The paddle was about 2 cm above the dialysis bag and rotated at 100 rpm. A weight settled the dialysis bag due to its tendency to float on the dissolution media when the paddle apparatus is employed. Samples of 3 mL were isolated at characteristic time intervals of 0.25, 0.5, 0.75, 1, 1.5, 2, 3, 4, 5, 10, 15, 20 and 24 hours and immediately replaced with equal volume of the fresh dissolution medium each time to preserve constant volume. The samples were evaluated for etoposide content by using a double beam UV-vis spectrophotometery. The drug released percentage was calculated via following equation:

$$D_{\%} = \frac{D_t}{D_0} \times 100\%$$

Where:

$D_{\%}$ is the drug release percentage at time t.

$D_0$ is the drug loaded amount in the formula.

$D_t$ is the drug release amount at certain time interval.[9]

The pH responsive capacity of E-GN suspensions was evaluated to investigate their feasibility to target cancer cells. Two dissolution medium of phosphate buffer pH=7.4 and acetate buffer pH=4.6 were used to study their effect on *in-vitro* etoposide release. In addition, the impact of temperature on the *in-vitro* etoposide dissolution profile at a particular pH=4.6 was investigated at a hyperthermic temperature 40°C.[7] All release studies were repeater in triplicates. The results were presented in mean value ± standard deviations.

## RESULTS AND DISCUSSION

### Preparation of Gold Nanoparticles

Inverse citrate reduction method was a more accurate, significant and reproducible procedure for preparation of GN due to seed mediated-growth mechanism.

GN suspension was transparent, clear, homogeneous and shiny with a stunning ruby red color; after about 27 minutes of preparation time. It was gave positive laser pointer and salt tests.[10] UV-vis spectrum of GN had a unique peak with absorbance maxima at 517 nm and narrow FWHM, as well as

higher size sensitive areas with lower shape sensitive areas, which indicated the presence of spherical GN with size less than 20 nm and uniform PSD.

AFM analysis of GN revealed a fine distribution of nanoparticles with smooth surface. The average PS was 8.75 nm with uniform SD (7.32%). These data supported the results of UV-vis analysis. A high negative zeta potential (-47.87) gave a steadiness, thus the suspension would be fighting versus aggregation.

**Functionalization of Gold Nanoparticles Suspension**

Development of the functionalized PGN suspensions necessitates preliminary work in order to obtain a clear transparent homogenous suspension, with positive laser pointer and negative salt tests. The perfect polymer coating of GN improves the colloidal stability and resists the effect of salt addition, minimizing the tendency of GN for aggregation and thereby giving a negative result for salt test. The phenomenon for polymer driving forces to improve the GN stability depends on the steric repulsion force between moieties of polymer; the moment that the polymer attached to the GN outer surface supplies sufficient repulsive potential, which can stabilize the dispersion. In the situation of nonionic polymers, the dispersion efficiency is high because of their hydrophilic similarity.[11]

PGN1-PGN5 and PGN9 with polymer concentrations lower than 0.5 mg/mL of HPMC-E5, HPMC-E15, poloxamer 188, poloxamer 407, PVA and gelatin, respectively, and lower than 0.25 mg/mL of PEG 200, PEG400 and PVP K30 for PGN6-PGN8 respectively, showed a positive salt test, which indicated for incomplete polymer coating. As well as revealed a dark red color immediately after preparation and then, turn into a blue suspensions within only one day, with a second UV-vis peak appeared at maximum absorbance more than 600 nm, which revealed to an aggregation process for the free GN.[7]

Nineteen polymeric suspensions (PGN1-19) were prepared by bioconjugation technique, using different polymers (of different molecular weight) with different concentrations, in order to screen for the preferable polymers with optimum concentration which improves the qualitative dispersibility measurements of GN suspension, as well as acceptable morphology, average PS and PSD.

Various conditions for preparation of the functionalized suspensions were investigated. Mixing the GN suspension with polymer solution at 25°C resulted in a suspension with good qualitative dispersibility measurements. Higher than this temperature gave a purplish-red suspension within a few minutes, indicating the formation of large aggregates. This clarifies that elevated the preparation temperature facilitated the kinetic of growth mechanism before the formation of polymer envelope.[12] Different sonication durations were utilized to screen for the optimum duration with acceptable qualitative dispersibility measurements. The optimum duration was found to be six hours, lower than this time resulted in an opaque pink suspension with positive salt test, which indicated the bad polymer coating during the bioconjugation process.[13]

PGN12 and PGN15 suspensions with higher concentration of polymer (20 mg/mL for HPMC-E5 and PVA, respectively), gave an opaque pink color, which indicated the formation of polymeric nanoparticles aggregates through intermolecular electrostatic interactions, in addition to loss of brightness with partial pass of laser pointer test due to loss of their uniformity.[14] PGN12 and PGN15 were rejected from the experiment.

Figures 1 and 2 demonstrate the AFM analysis of the functionalized suspensions PGN1-PGN9 with various polymers types and their molecular weights. Increasing the PS of GN with uniform PSD, after mixing with polymer solution, confirmed that GN were actually conjugated with the polymer via coordination bonds.[15] The AFM analysis of the functionalized suspensions with different polymers types showed that the GN size and their distribution increased significantly ($p < 0.05$) with increasing the molecular weight of polymers used. These results could be related to increase the conformational entropy and steric hindrance of polymer with increasing in the polymer chain length.[16]

AFM analysis of PGN6-PGN8 suspensions prepared from PEG 200, PEG 400 and PVP 30K respectively, which revealed a larger PS with bad uniformity that indicated for failure of these polymers to improve the colloidal stability of GN. The reason behind these results might be related to the samples preparation process, since PGN6-PGN8 were a sticky nanoparticles suspensions therefore, their AFM samples needed about five days to dry at 25°C, this time is enough to form a large aggregates of GN through a growth mechanism.[17]

PGN1, PGN5 and PGN9 suspensions that were prepared from HPMC-E5, PVA and gelatin, respectively, gave a lower PS and better PSD. The uniformity of polymeric suspensions gave an indication for the uniformity of a stable polymer coating during bioconjugation process. Therefore HPMC-E5, PVA and gelatin were selected as preferable polymers for further studies.

The AFM analysis of PGN10-PGN18 suspensions, as illustrated in Figure 3, showed complex relationship between the concentration of polymer and the reduction of nanoparticles size. The PS and PSD was significantly decreased ($p<0.05$) by increasing the concentration of polymer from 0.5 to 1-mg/mL for HPMC-E5 and PVA, and to 1.5 mg/mL for gelatin, then the final particles size and size distribution started to increase significantly ($p<0.05$) above these concentrations. The non-linear concentration dependence occurred due to decrease the free GN with increasing concentration of polymer, which led to decrease the possible small GN aggregates via coordination bonds. While increasing the concentrations of polymer more than the optimum limit leading to large aggregates formation of individual PGN by inter-molecular electrostatic interactions.[7]

The AFM analysis of PGN12 and PGN15 with higher concentration of polymer of 20 mg/mL for HPMC-E5 and PVA, respectively, revealed large aggregates of polymeric nanoparticles with very large PSD, which supported the results of qualitative dispersibility measurements that mentioned previously.

PGN19 suspension that was prepared from combination of the two preferable polymers HPMC-E5 and PVA with similar best concentration of 1mg/mL, at ratio 1:1, revealed the smallest final nanoparticles size (average PS 13.25 nm)

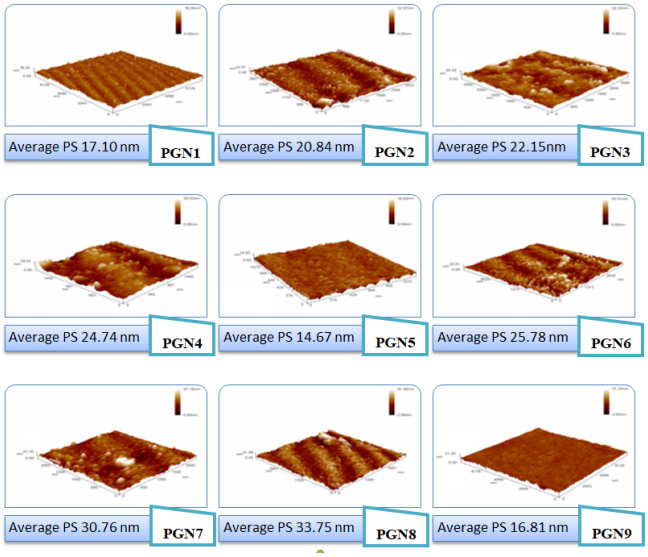


**Figure 1:** AFM 3D images of PGN1-PGN9

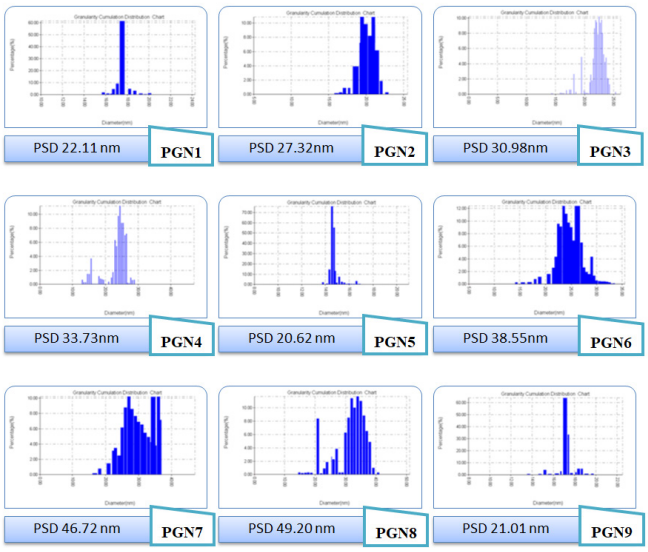


**Figure 2:** AFM particles size distribution of PGN1-PGN9

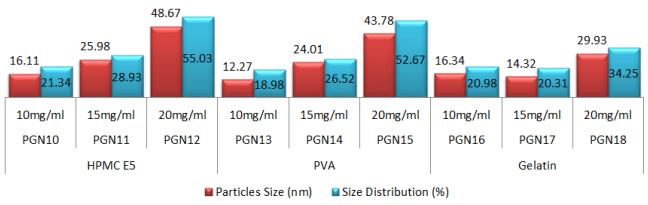


**Figure 3:** AFM analysis of PGN10-PGN18

with a best PSD (18.11%) when compared with the suspensions of each polymer separately, confirmed that this combination enhanced the polymer coating tendency for stabilization the GN by improvement of the electrostatic repulsion forces, as shown in Figure 4.[18]

The functionalized suspensions PGN10, PGN13, PGN17 and PGN19 with the preferable polymers and their concentration of (1-mg/mL HPMC E5, 1-mg/mL PVA, 1.5 mg/mL gelatin and 0.5: 0.5 mg/mL of HPMC E5: PVA combination) respectively,

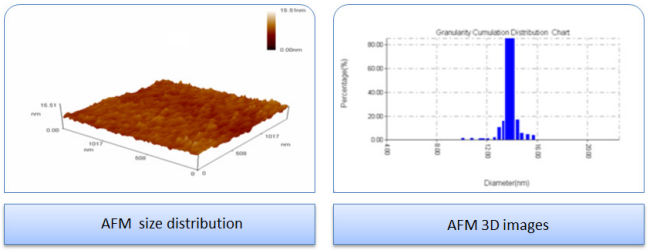


**Figure 4:** AFM Analysis of PGN19

showed the better morphology, PS, and PSD, which were selected for further studies.

The compatibility between etoposide and various polymers (HPMC-E5, PVA or gelatin) used in preparing the E-GN suspensions were detected, to confirm no interaction between etoposide and polymers.

FTIR (Figure 5) is very powerful spectroscopic technique and one of the most widely reported drug-excipients compatibility studies for solid-state characterization. The characteristic absorption band of etoposide showed a strong absorbance band at 3400 $cm^{-1}$, which is related to the stretching of phenolic OH group. While the characteristic band for the C-O-C stretching appeared at 1250 $cm^{-1}$, bands at 1610, 1515 and 1485 $cm^{-1}$ are corresponding to aromatic C=C stretching. The characteristic absorption band at 1775 $cm^{-1}$ with strong stretching intensities is attributed to presence of the lactone group; these are the main characteristic absorption bands of etoposide.[19]

HPMC-E5 is a semisynthetic nonionic polymer. The characteristic band of strongly associated OH vibration appeared at 3450 $cm^{-1}$ and C-O-C group at 1056 $cm^{-1}$, as well as asymmetric and symmetric C-H stretching bands appeared at 2930 and 2840 $cm^{-1}$, respectively.[20]

PVA is a synthetic nonionic polymer. The characteristic band of strongly associated OH vibration appeared at 3290 $cm^{-1}$ and C-O stretching vibration at 1141 and 1081 $cm^{-1}$, as well as $CH_X$ vibrations can be discerned at 1417, 2906 and 2945 $cm^{-1}$.[21]

Gelatin is a natural cationic polymer. The characteristic bands of amide C=O stretching vibrations appeared at 1630, 1521 and 1235 $cm^{-1}$ and amide N-H stretching band at 3275 $cm^{-1}$, bands at 1444, 1334, 2873 and 2934 $cm^{-1}$ corresponding to $CH_X$ vibrations.[21]

The spectra of physical mixtures of etoposide: HPMC-E5, etoposide: PVA and etoposide: gelatin at ratio 1:1 were equivalent to the spectra of etoposide and polymers indicating no chemical interaction or complexation formation in physical mixture of etoposide and the polymers.

*Preparation of E-GN*

Developing the E-GN suspensions necessitates preliminary work to study the effect of several variables to improve the etoposide LE.

The LE of suspensions containing a cationic gelatin was enhanced significantly ($p<0.05$) by increase the initial pH of etoposide solution above its pka value, this is attributed to the effect of ionization. On the other hand, the etoposide

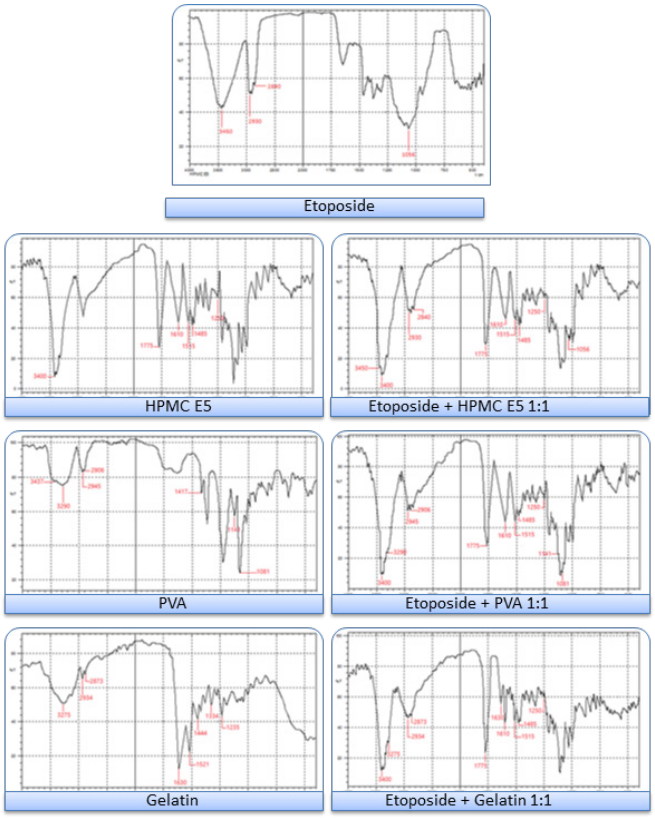


**Figure 5:** FTIR spectra

**Table 3:** Etoposide LE of F3-F8

| *Formula code* | *Polymer type* | *LE%* |
|---|---|---|
| F3 | | 91.73 |
| F5 | Gelatin | 64.43 |
| F6 | | 37.01 |
| F4 | | 88.21 |
| F7 | HPMC-E5:PVA | 99.39 |
| F8 | | 77.93 |

LE of suspensions containing non ionic HPMC-E5 or PVA was not significant affected ($p>0.05$) by change the initial pH of etoposide solution.which is attributed to the stability of etoposide aqueous solution at acidic condition of pH 4-5, that is contributed to the enhancement of etoposide adsorption on the surface of polymeric gold nanoparticles. The reason behind this result was thought to be attributed to the behavior of etoposide molecules in the buffer solution of pH 7.4. It's known that etoposide is a weak base with pka 9.8, so when pH decreased below pka value the ratio of ionized [$BH^+$] to non-ionized [B] species increased according to Henderson-Hassel Balch equation. Therefore at pH 7.4, etoposide molecules are almost fully protonated [$BH^+$] and interact with the only few negatively charged carboxyl groups of cationic gelatin layer of gold nanoparticles. On the other hand, at pH above pka, etoposide molecules are deprotonated [B], which promotes the electrostatic interaction with a positively charged gelatin layer.[22, 23]

Etoposide solutions at pH=10.5 with concentration >5 mg/mL turn in to cloudy solution after about 30 minutes. of preparation, also at pH>5 the aqueous etoposide solution became less stable,[23] and thus for gelatin coating gold nanoparticles, it must be prepared freshly via the incorporation method.

The etoposide LE of suspensions containing gelatin was improved significantly ($p<0.05$) by elevating the incorporation temperature within a certain limit of (not above 55°C), which is related to lower viscosity and higher kinetic energy of gelatin protecting layer by increasing the temperature condition at pH environment other than its isoelectric point (pH=4.7), this led to enhancement of etoposide adsorption through electrostatic interactions.[7] On the other hand, the etoposide LE of suspensions containing HPMC-E5 or PVA was significant decreased ($p<0.05$) with increasing the incorporation method temperature. The reason for this result was that the polymers chains conformation in aqueous solution be higher stretched at elevated temperature, leading to decreased etoposide adsorption on the surface of PGN.[24]

Eight formulas of E-GN were prepared via incorporation method. Various biocompatible polymers (HPMC-E5, PVA, gelatin or HPMC-E5: PVA) have been used for functionalization of GN to improve their capacity of payloads, stability and cellular uptake.[8]

PNG with ultra nano-size could allow a large surface area for incorporation of etoposide. Besides the existence of surface active groups (amide, carboxyl or hydroxyl), these nanoparticles have a large loading capacity, which might enhance the bonds formation with etoposide per unit surface area.[25]

The polymer type effect on E-GN was evaluated using HPMC-E5, PVA, gelatin and HPMC-E5: PVA combination for formulas (F1-F4) respectively. All formulas were clear, transparent and homogeneous, with glossy red color indicated for the stability of suspended E-GN.[7]

The PS has an impact on the LE of etoposide. The observation suggested that LE of E-GN was enhanced with the reduction in the PS. As a well known fact; "lower the particle size more will be the availability of surface containing active sites for adsorption of drug".[26] Therefore, the etoposide LE for the PGN was enhanced by using various types of polymers and it was found in the following order:

HPMC-E5: PVA combination > PVA > HPMC-E5 > gelatin as presented in (F4, F2, F1 and F3), respectively.

The dissolution profile of formula F1 consisting of HPMC-E5 appeared a very low etoposide dissolution rate in both dissolution medium of phosphate buffer pH=7.4 and acetate buffer pH=4.6 (less than 20% of etoposide released after 24 hours), which could be linked to the polymer stability under the medium pH change, producing elevated retardation of drug release. Otherwise the dissolution profile of formula F2 consisting of a pH-sensitive polymer (PVA) revealed a lower etoposide retarding at phosphate buffer pH=7.4 and extremely dissolution rate at acetate buffer pH=4.6 with burst released the active component through <15 minutes.[27]

The etoposide LE of formulas containing HPMC-E5 and PVA combination which was significantly ($p<0.05$) larger than

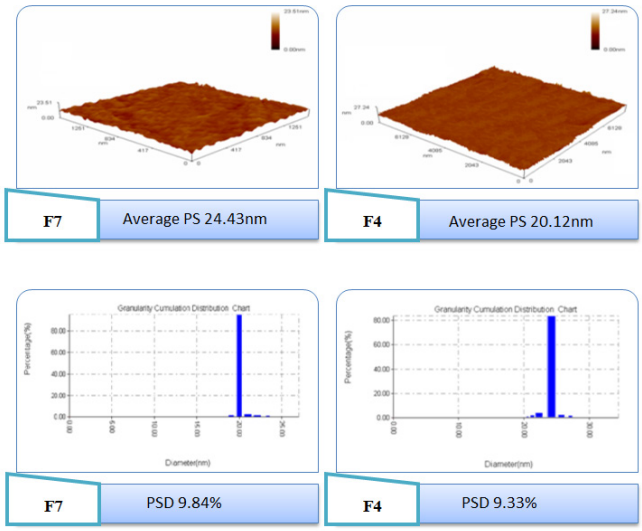


**Figure 6:** AFM analysis of F4 and F7

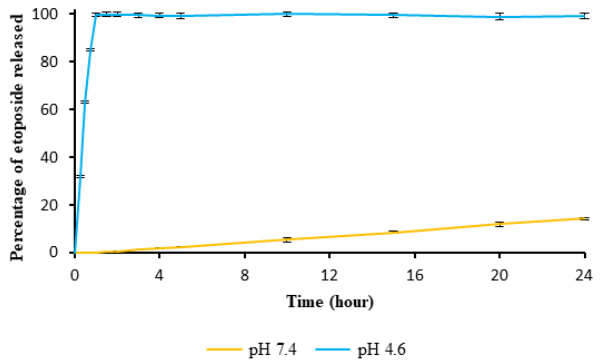


**Figure 7:** Etoposide dissolution profile from formula F7 in phosphate (pH=7.4) and acetate (pH=4.6) buffer solutions at 37±1°C (data represented as mean%±SD, n=3)

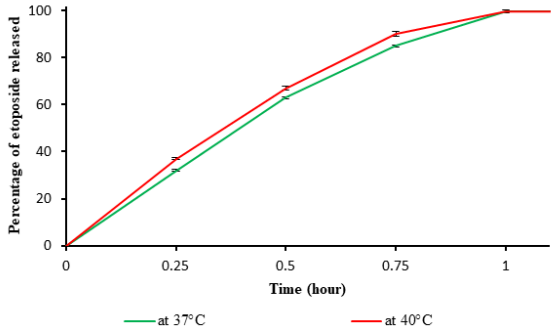


**Figure 8:** Etoposide dissolution profile from formula F7 in acetate buffer solution (pH=4.6) at 37 and 40 ± 1°C (data represented as mean% ± SD, n=3)

those containing gelatin with all different initial etoposide loading of (5, 10 and 15 mg/mL), indicating the greater capacity of HPMC-E5: PVA combination layer for etoposide adsorption, as shown in Table 3. Formulas F3, F5 and F6 prepared from gelatin coated GN were rejected from the study. The maximum loading capacity of (10 mg/mL etoposide solution) with higher LE of (more than 99%) appeared in Formula F7, containing

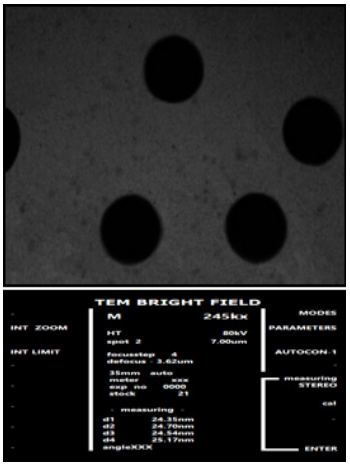


**Figure 9:** TEM image of F7

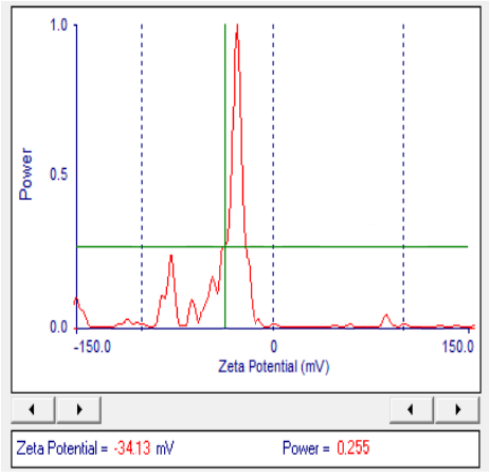


**Figure 10:** Zetapotential monograph of F7

HPMC-E5: PVA combination. However formula F8 prepared from HPMC-E5: PVA combination with higher concentration of etoposide solution (15 mg/mL) gave a lower etoposide LE, so it was also rejected from the study.

The AFM analysis, as shown in Figure 6, which appeared a significantly increased ($p<0.05$) in particles size of formula F7 with concentration 10 mg/mL of etoposide solution, in comparison with formula F4 with lower concentration of 5 mg/mL,that proved the greater capacity of HPMC-E5 and PVA combination layer for etoposide adsorption. On the other hand, no significantly difference ($p>0.05$) in etoposide dissolution profiles was attained by increasing the etoposide loading for these formulas.[7]

The dissolution profile (Figure 7) of formula F7 revealed a preferable retardation of etoposide at phosphate buffer pH=7.4 and better dissolution rate with controlled mode at acetate buffer pH=4.6.[7]

Figure 8 illustrates the impact of temperature on the *in-vitro* etoposide dissolution profile, of the optimized formula F7, at a particular pH=4.6. It was found a significant improvement ($p<0.05$) in etoposide dissolution profiles at a hyperthermic temperature 40°C.[8]

The TEM image of F7 showed uniform spherical nanoparticles,[28] with average PS of 24.69 nm, as in Figure 9. These data were inconsistent with the data of AFM analysis of 24.43 nm, since statistically, there is no significantly ($p>0.05$) difference between them.

Zeta potential is the electrostatic potential which presents at the particle share plane and linked to the surface charge as well as the local environment of particles.[29] F7 revealed a highly negative zeta potential of -34.13, as shown in Figure 10, indicating their stability in the suspensions. The higher electric surface charge would prevent aggregation of E-GN in buffer solution due to strong repellent forces between particles.[30]

## CONCLUSION

Polymeric functionalization of gold nanoparticles enhanced the colloidal stability, improved the etoposide loading efficiency and capacity, and controlled the *in-vitro* dissolution profile. E-GN developed from the functionalized GN with a combination of HPMC-E5 and PVA (1:1) showed better nanoparticles size and shape uniformity, maximum etoposide LE and controlled release.

The results show that etoposide loaded-gold nanoparticles were a credible candidate to be a successful multiplexed pharmaceutical agent. Thus, I promote further study expansion, including evaluating the toxicity studies and pharmacokinetic profile.

## REFERENCES


1. Bandopadhyay, S.; Manchanda, S.; Chandra, A.; Ali, J.; Deb, P.K. Overview of different carrier systems for advanced drug delivery. In: *Drug Delivery Systems*. Academic Press 2020, pp. 179-233. https://doi.org/0.1016/B978-0-12-814487-9.00005-3
2. Fu, L.H.; Yang, J.; Zhu, J.F.; Ma, M.G. Synthesis of gold nanoparticles and their applications in drug delivery. In: *Metal Nanoparticles in Pharma*. Springer, Cham 2017, pp. 155-191. http://dx.doi.org/10.1007/978-3-319-63790-7_9.
3. O'NEIL, M.J. The Merk Index: An Encyclopedia of Chemicals, Drugs and Biological. 15th Edition. *Royal Society of Chemistry* 2013.
4. Khalid, N.; Sarfraz, M.; Arafat, M.; Akhtar, M.; Löbenberg, R.; Rehman, N.U. Nano-sized droplets of self-emulsifying system for enhancing oral bioavailability of chemotherapeutic agent VP-16 in rats: A nano lipid carrier for BCS class IV drugs. *Journal of Pharmacy and Pharmaceutical Sciences* 2018, 21: 398-408. https://doi.org/10.18433/jpps30097
5. Turkevich, J.; Stevenson, P.C.; Hillier, J. A study of the nucleation and growth processes in the synthesis of colloidal gold. *Discussions of the Faraday Society* 1951, 11: 55-75.
6. Islam, Z.A.; Mondal, S.; Islam, M. Applications, synthesis and characterization of gold nano particles. PhD Thesis. *BRAC Univeristy, Dhaka* 2017. http://hdl.handle.net/10361/8614
7. Suarasan, S.; Focsan, M.; Potara, M.; Soritau, O.; Florea, A.; Maniu, D.; Astilean, S. Doxorubicin-incorporated nanotherapeutic delivery system based on gelatin-coated gold nanoparticles: formulation, drug release, and multimodal imaging of cellular internalization. *American Chemical Society Applied Materials & Interfaces* 2016, 8: 22900-22913. https://doi.org/10.1021/acsami.6b07583, https://doi.org/10.4274/tjps.galenos.2018.21043
8. Farooq, M.U.; Novosad, V.; Rozhkova, E.A.; Wali, H.; Ali, A.; Fateh, A.A.; Neogi, P.B.; Neogi, A.; Wang, Z. Gold nanoparticles-enabled efficient dual delivery of anticancer therapeutics to HeLa cells. *Scientific Reports* 2018, 8(1): 1-12. https://doi.org/10.1038/s41598-018-21331-y, https://doi.org/10.1016/j.ijbiomac.2016.06.007
9. Madhusudhan, A.; Reddy, G.B.; Venkatesham, M.; Veerabhadram, G.; Kumar, D.A.; Natarajan, S.; Yang, M.; Hu, A.; Singh, S.S. Efficient pH dependent drug delivery to target cancer cells by gold nanoparticles capped with carboxymethyl chitosan. *International Journal of Mechanical Sciences* 2014, 15: 8216-8234. https://doi.org/10.3390/ijms15058216
10. Babaei Afrapoli, Z.; Faridi, Majidi, R.; Negahdari, B.; Tavoosidana, G. 'Reversed Turkevich' method for tuning the size of Gold nanoparticles: evaluation the effect of concentration and temperature. *Nanomedicine Research Journal* 2018, 3(4): 190-196. https://dx.doi.org/10.22034/nmrj.2018.04.003
11. Napper, D.H. Steric stabilization. *Journal of Colloid and Interface Science* 1977, 58(2): 390-407. https://doi.org/10.1016/0021-9797(77)90150-3
12. Zhou, J.; Ralston, J.; Sedev, R.; Beattie, D.A. Functionalized gold nanoparticles: synthesis, structure and colloid stability. *Journal of Colloid and Interface Science* 2009, 331(2): 251-262. https://doi.org/10.1016/j.jcis.2008.12.002
13. Chuang, C.C.; Cheng, C.C.; Chen, P.Y.; Lo, C.; Chen, Y.N.; Shih, M.H.; Chang, C.W. Gold nanorod-encapsulated biodegradable polymeric matrix for combined photothermal and chemo-cancer therapy. *International Journal of Nanomedicine* 2019, 14: 181-193. https://doi.org/10.2147/IJN.S177851
14. Ende, V.E.; Bourgeois, M.C.; Henry, A.I.; Chávez, J.L.; Krabacher, R.; Schatz, G.C.; Van Duyne, R.P. Physicochemical Trapping of Neurotransmitters in Polymer-mediated Gold Nanoparticle Aggregates for Surface-enhanced Raman Spectroscopy. *Analytical Chemistry,* 2019, 91(15): 9554-9562. https://doi.org/10.1021/acs.analchem.9b00773
15. Lay-Ekuakille, A.; Spano, F.; Mvemba, P.K.; Massaro, A.; Galiano, A.; Casciaro, S.; Conversano, F. Conductivity Image Characterization of Gold Nanoparticles based-Device through Atomic Force Microscopy. In: *2018 Nanotechnology for Instrumentation and Measurement (NANOfIM)*. IEEE 2018, pp. 1-6. https://doi.org/10.1109/NANOFIM.2018.8688617
16. Rahme, K.; Chen, L.; Hobbs, R.G.; Morris, M.A.; O'Driscoll, C.; Holmes, J.D. PEGylated gold nanoparticles: polymer quantification as a function of PEG lengths and nanoparticle dimensions. *Rsc Advances* 2013, 3(17): 6085-6094. https://doi.org/10.1039/c3ra22739a
17. Michen, B.; Geers, C.; Vanhecke, D.; Endes, C.; Rothen-Rutishauser, B.; Balog, S.; Petri-Fink, A. Avoiding drying-artifacts in transmission electron microscopy: Characterizing the size and colloidal state of nanoparticles. *Scientific reports* 2015, 5: 9793. https://doi.org/10.1038/srep09793
18. Madkour, M.; Bumajdad, A.; Al-Sagheer, F. To what extent do polymeric stabilizers affect nanoparticles characteristics?. *Advance in Colloid Interface Science* 2019, 270: 38-53. https://doi.org/10.1016/j.cis.2019.05.004
19. Partani, R.; Kasturi, M.; Malviya, N. Enhancement of Aqueous Solubility of Etoposide Using Solid Dispersion Technique. *Research & Reviews: A Journal of Pharmacology* 2019, 9(1): 29-37. http://pharmajournals.stmjournals.in/index.

php/RRJoP/article/view/237

20. Sheikh, F.A.; Aamir, M.N.; Shah, M.A.; Ali, L.; Anwer, K.; Javaid, Z. Formulation design, characterization and in vitro drug release study of orodispersible film comprising BCS class II drugs. *Pakistan Journal of Pharmaceutical Sciences* 2020, 33(1): 343-353. https://doi.org/10.36721/PJPS.2020.33.1.SUP.343-353.1
21. Sudhamani, S.R.; Prasad, M.S.; Sankar, K.U. DSC and FTIR studies on gellan and polyvinyl alcohol (PVA) blend films. *Food Hydrocolloids* 2003, 17(3): 245-250. https://doi.org/10.1016/S0268-005X(02)00057-7
22. Brayfield, A. Martindale: The Complete Drug Reference. 39th Edition. *Pharmaceutical Press* 2017.
23. Kosjek, T.; Negreira, N.; Heath, E.; de Alda, M.L.; Barceló, D. Biodegradability of the anticancer drug etoposide and identification of the transformation products. *Environmental Science and Pollution Research* 2016, 23(15): 14706-14717. https://doi.org/10.1007/s11356-016-6889-5
24. Wiśniewska, M. Temperature effects on the adsorption of polyvinyl alcohol on silica. *Open Chemistry* 2012, 10(4): 1236-1244. https://doi.org/10.2478/s11532-012-0044-z
25. Kong, F.Y.; Zhang, J.W.; Li, R.F.; Wang, Z.X.; Wang, W.J.; Wang, W. Unique roles of gold nanoparticles in drug delivery, targeting and imaging applications. *Molecules* 2017, 22: 1445, 1-13. https://doi.org/10.3390/molecules22091445
26. Devrim, B.; Canefe, K. Preparation and evaluation of modified release ibuprofen microspheres with acrylic polymers (eudragit) by quasi emulsion solvent diffusion method: Effect of variables. *Acta Poloniae Pharmaceutica - Drug Research* 2006, 63(6): 521-534. http://www.ptfarm.pl/pub/File/Acta_Poloniae/2006/6/521.pdf
27. Sabzi, M.; Afshari, M.J.; Babaahmadi, M.; Shafagh, N. PH-dependent swelling and antibiotic release from citric acid crosslinked poly (vinyl alcohol) (PVA) / nano silver hydrogels. *Colloids and Surfaces B: Biointerfaces* 2020, 188: 110757. https://doi.org/10.1016/j.colsurfb.2019.110757
28. Mohamed, A.I.; Hussain, A.K.; Zayed, G.M.; Shaykoon, S.M.; Mahmoud, R.A. Preparation and characterization of cytotoxic drug loaded gold nanoparticles. *International Journal of Pharmacy and Pharmaceutical Research* 2016, 6(4): 640-652.
29. Pinton, A.P.; de S Bulhões, L.O. Synthesis, characterization, and photostability of manganese-doped titanium dioxide nanoparticles and the effect of manganese content. *Materials Research Express* 2019, 6(12): 125015, 1-9. https://doi.org/10.1088/2053-1591/ab533b
30. Reznickova, A.; Slavikova, N.; Kolska, Z.; Kolarova, K.; Belinova, T.; Kalbacova, M.H., Belinova, T.; Kolarova, M.H.; Cieslar, M.; Svorcik, V. PEGylated gold nanoparticles: Stability, cytotoxicity and antibacterial activity. *Colloids and Surfaces A: Physicochemical and Engineering Aspects* 2019, 560: 26-34. https://doi.org/10.1016/j.colsurfa.2018.09.083